A powdered orange peel combined carboxymethyl chitosan and its acylated derivative for the emulsification of marine diesel and 2T-oil with different qualities of water

Doshi, Bhairavi

2019-10-01

Doshi , B , Hietala , S , Sirviö , J A , Repo , E & Sillanpää , M 2019 , ' A powdered orange peel combined carboxymethyl chitosan and its acylated derivative for the emulsification of marine diesel and 2T-oil with different qualities of water ' , Journal of Molecular Liquids , vol. 291 , 111327 . https://doi.org/10.1016/j.molliq.2019.111327

http://hdl.handle.net/10138/306050
https://doi.org/10.1016/j.molliq.2019.111327

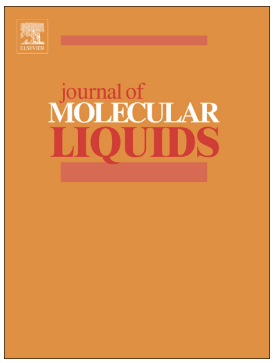

A powdered orange peel combined carboxymethyl chitosan and its acylated derivative for the emulsification of marine diesel and 2T-oil with different qualities of water

Bhairavi Doshi, Sami Hietala, Juho Antti Sirviö, Eveliina Repo, Mika Sillanpää

PII: S0167-7322(19)31756-8
DOI: https://doi.org/10.1016/j.molliq.2019.111327
Article Number: 111327
Reference: MOLLIQ 111327

To appear in: *Journal of Molecular Liquids*

Received date: 26 March 2019
Revised date: 11 June 2019
Accepted date: 6 July 2019

Please cite this article as: B. Doshi, S. Hietala, J.A. Sirviö, et al., A powdered orange peel combined carboxymethyl chitosan and its acylated derivative for the emulsification of marine diesel and 2T-oil with different qualities of water, Journal of Molecular Liquids, https://doi.org/10.1016/j.molliq.2019.111327

A powdered orange peel combined carboxymethyl chitosan and its acylated derivative for the emulsification of marine diesel and 2T-oil with different qualities of water

Bhairavi Doshi,[a,*] Sami Hietala,[b] Juho Antti Sirviö,[c] Eveliina Repo,[d] Mika Sillanpää,[a]

[a] Department of Green Chemistry, LUT University, Sammonkatu 12, FI-50130 Mikkeli, Finland

[b] Department of Chemistry, University of Helsinki P.O. Box 55, FIN-00014

[c] Fibre and Particle Engineering Research Unit, University of Oulu, P.O. Box 4300, FI-90014, Finland

[d] Department of Separation and Purification, School of Engineering Science, LUT University, Yliopistonkatu 34, FI-53850, Finland

[*] **Corresponding Author**

Email: bhairavi.doshi@lut.fi; bhairavidoshi3@gmail.com; Phone: +358504356962

Abstract

The traces of hazardous chemicals used in oil spill response have harmed marine creatures with long-term cytoxic impacts, so, a greener alternative is to use biodegradable components in the dispersant formulation. This study demonstrates the efficiency of carboxymethylated and acylated chitosan combined with powdered orange peel (OP-D) in the emulsification of marine diesel and 2T-oil with different qualities of water. OP-D particles undergo Pickering emulsions, whereas the amphiphilic behaviour of the Blend and hydrophobically modified carboxymethyl chitosan-orange peels (CSOP-A) favours conventional emulsions through steric and electrostatic stabilization. The emulsion formation rate was maximum with OP-D in saline water and autonomous of the water quality with Blend. Additionally, different hydrophobic moieties on the surface of the Blend and CSOP-A affected the oil droplets' stabilization rate. Changing pH altered the surface properties of particles and hence the nature of the formed emulsion range from gel-like to creamy, suggesting particle-particle to particle-oil interactions. An increase in electrolyte concentration enhanced the coalescence rate of marine diesel with CSOP-A. The oil droplet size in the formed emulsion increases with a temperature decrease up to 2°C, and the emulsion stabilization rate was less than 10% at -20°C. The traces of these synthesized materials were less than 1000 mg L^{-1} in the water phase after the removal of oils. Since these materials are bio-based, their presence in the ecosystem is less hazardousness than commercial dispersants.

Keywords

Orange peel powder; modified chitosan; hydrophobic modification; emulsion stabilization; water quality; electrosteric stabilization.

1. INTRODUCTION

After a number of oil spill incidents such as Deepwater Horizon in the Gulf of Mexico and Exxon Valdez in Alaska, various rules, regulations and strategies have been enacted to control such spills in the future. Currently, various techniques such as mechanical methods, bio-remediation, in-situ burning and dispersants are applied to oil spill response, depending on the climatic conditions. In the Arctic region, chemical herders forming thick oil slicks are key to effective in-situ burning [1], but the fracturing of oil during the herding process in the presence of ice reduces burning efficiency [2]. Secondly, the type of oil and its behaviour with ice and saline water also play a significant role in dispersant efficiency [3]. Although chemical dispersants have enhanced the biodegradation of spilled oil by reducing oil droplet size, these dispersants in water resources were cytotoxic for marine creatures [4,5]. Recently, many alternative eco-friendly dispersants based on food-grade amphiphiles have been studied [6,7]. In addition, oil emulsifiers based on biopolymers such as cellulose [8,9], chitosan [10,11], and xanthan gum [12] have been studied extensively for oil spill response.

Chitin found in the shells of crustaceans and molluscs is the second most abundant natural polymer [13,14], a major source of surface pollution in coastal areas and a waste material in seafood production industries [15]. Therefore, the utilization of leftover chitin would reduce the amount of sea waste [16]. Chitosan is the deacetylated form of chitin and widely used as a biomaterial and a sorbent, because of its diverse surface properties. The surface-active functional groups of chitosan can be modified by various methods such carboxyalkylation, acylation, alkylation, cross-linking, grafting and ionic-gelation, which can be effectively used in oil spill treatment [17]. Despite chemical modification, the fundamental skeleton remains intact in modified chitosan, which retains its original physicochemical and biochemical properties, and incorporates improved properties. Amphiphilic chitosan can be used as a surfactant, either in the form of a dispersing or herding agent. Recently, chitosan-based bio-polymeric blends [18] and magnetic nanoparticles [19,20] have also been studied for the removal and/or separation of oil from water resources.

Emulsion droplet stabilization is often achieved through the addition of amphiphilic molecules such as surfactants or emulsifiers, which decrease interfacial tension between the phases and increase steric hindrances and/or electrostatic repulsion between the droplets [21]. Furthermore, the emulsion

stabilization also depends on particle concentration and particle-particle interactions [22]. Chitosan and modified chitosan produce stabilized conventional emulsions, where dissolved materials provides a steric barrier against coalescence of the oil droplets due to weak surface activity [23,24]. So far, the Pickering emulsions have attracted more interest in the field of nanoparticles, as they form kinetically stable emulsions through a physical barrier and not by decreasing the tension between the phases. In other ways, particles undergo Pickering emulsions via irreversible adsorption at the liquid-liquid interface to stabilize emulsions [21,25,26]. On the other hand, French et al. showed the exchange of particles between the droplets in Pickering emulsion [27]. The particles must be small enough for effective Pickering emulsion and to regulate the size of the oil droplets, while larger particles will improve steric hindrance and prevent coalescence [22,28,29]. The adsorbed surface-active particle at the interface provides electrostatic or steric barriers against coalescence, and thus enhance the emulsion stability.

A large amount of food waste (lignocellulosic-rich) is generated by agricultural and various food industries, and nearly 15.6 million tonnes of waste comes from citrus fruit peel [30]. This peel is rich in nutrients [31,32] and could be effectively applied in wastewater remediation [33–35] and many other alternative sustainable technologies [36–38]. Orange peel (OP) is composed of flavonoids, phenolics, carotenoids, pectin, lignin, cellulose, hemicellulose, limonene, soluble sugars, oil and fat [39]. The esterification of sugars (such as sucrose) [40] and flavonoids [41] by acid chlorides acts as a surfactant. Abudullah et al. demonstrated the removal of oil from saline water using orange peel, but its removal efficiency decreased with decreasing salinity [42]. Previously, we demonstrated the destabilization of marine diesel up to seawater salinity using a sodium form of chitosan derivative [43] but, to the authors' knowledge, the combined derivative of chitosan and orange peel has not yet been studied for the stabilization of oil.

The objective of conducting this study was to demonstrate the valorization of orange peel (OP) together with modified chitosan as surface-active particles and/or an emulsifier. These materials undergo hydrophobic modification via acylation, and are used to stabilize marine diesel and 2T-oil present on the water surface. The synthesized materials were characterized using a Fourier transform infrared spectrophotometer (FTIR), Proton nuclear magnetic resonance spectroscopy (^{1}H NMR), X-ray diffraction spectroscopy (XRD), Brauner, Emmet and Teller analysis (BET), Elemental analysis (EA), Scanning electron microscopy (SEM), Energy dispersive X-ray spectroscopy (EDS) and surface charge. The droplets stabilization rate of oils was studied using these materials with deionized and saline water.

The emulsion behaviour of marine diesel and 2T-oil was also investigated as a function of solution pH and salinity. As these oils have different densities and composition, their stabilization rate varied. We used visual observations and optical microscopy to study the oil droplets formed due to the stabilization of oils. We also investigated the nature of the oil droplets with varying temperature, and furthermore, we studied the total organic carbon (TOC) amount of these derivatives in water using the non-purge organic carbon (NPOC) method after the removal of oils/emulsified oils.

2. MATERIAL AND METHODS

2.1 Materials

Chitosan (from shrimp shells), acetone, oleoyl chloride (C18), lauroyl chloride (C12), hydrochloric acid (HCl), sodium hydroxide (NaOH) and ethanol were obtained from Sigma Aldrich Oy and Altia Oyj. All chemicals were used without further purification. OP waste was collected from oranges purchased from the local market. Marine diesel and 2T-oil were purchased from Neste Oyj, Finland. Deionized water (DI) was used throughout the experiments and saline water was collected from the area near Matinkylä Espoo, Finland.

2.2 Synthesis of powdered orange peels, hydrophobically modified carboxymethyl chitosan-orange peels and the Blend

Chitosan-based materials, sodium form of carboxymethyl chitosan (Na-CMCS) and sodium form of carboxymethyl oleoyl chitosan (NaO-CMCS) were synthesized as per our previous studies [43]. The synthesis routes (SR) are shown in Figure 1.

In SR1, orange peel was washed and dried at room temperature (RT) for 48 h. This dried orange peel was ground in a tubemill and dried again for 24 h at 60°C making powdered orange peel (OP-D). In SR2, equal portions of OP-D and NaO-CMCS were mixed to get the Blend. In SR3, the mixture of Na-CMCS (1.2 g) and OP-D (1.1 g) was soaked in acetone (20 mL) for 1 h at 5°C. To this mixture, lauroyl chloride in acetone (1:1, 2.6 mL each) and NaOH solution (4 M) were added simultaneously after 30 min, and stirred continuously for 4 h at the same temperature. Ethanol (70%) was then added to the reaction mixture. The obtained solid was washed three times with ethanol (70–90%), dried overnight at RT and ground in the tubemill. This obtained dried solid is hydrophobically modified carboxymethyl chitosan-orange peel (CSOP-A).

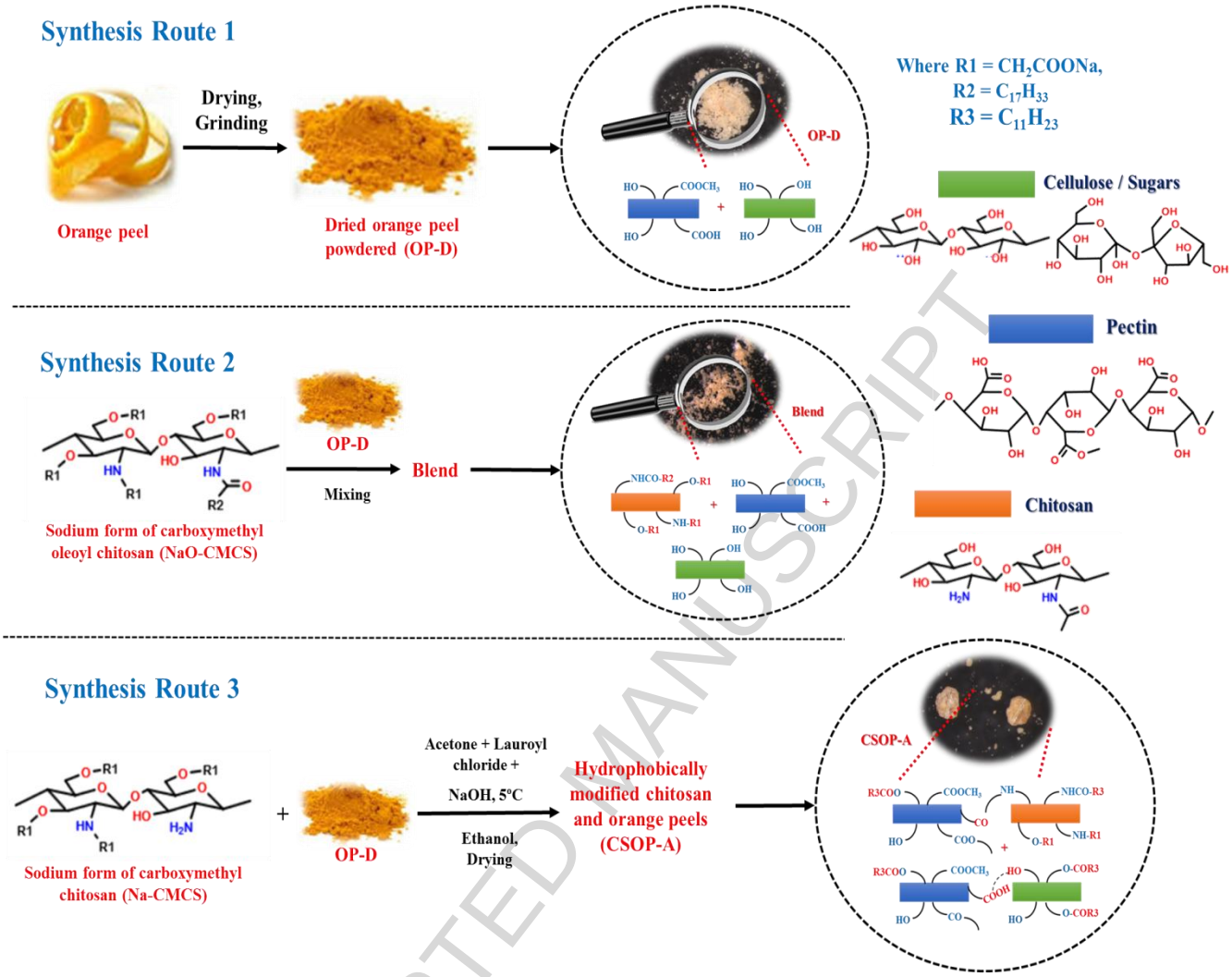

Figure 1: Schematic of OP-D, Blend and CSOP-A synthesis along with the structural and functional change.

2.3 Characterization

The synthesized materials were characterized using FTIR, SEM/EDS, XRD, ^{1}H NMR, elemental analysis, BET, and surface zeta potential (ZP). The interfacial tension between the oil and aqueous phases was also determined using these materials. The details about the characterization methods are available in SM1.

2.4 Effect of dosage and solution pH on the emulsion formation rate

The emulsion formation rate was studied by mixing 10 mL (0–2.5 g L^{-1}) of synthesized materials solutions in DI and SW, respectively, with an oil-to-water ratio of 0.1, so the material-to-oil-ratio would

range from 0 to ~0.03 depending on the type of oil (Refer SM2). The mixing was conducted in a centrifuge tube (15 mL) with a test tube shaker (Heidolph) at 2000 rpm for 1 min. After mixing, these solutions were rested for a day to evaluate the stabilization rate, i.e. the emulsion formation rate (see equation 1). The oil droplet size in the emulsion formed was also measured with an optical microscope (Zeiss Axio using the 206-camera unit Axio CamERc5s with ZEN software). Similarly, the effect of pH ranging from 3.5–10.5 was investigated in the stabilization rate with the optimized dosage (from the above studies). The amount of separated oil was measured simultaneously to determine the coalescence rate (see equation 2) of oil after mixing and resting. This optimized concentration and solution pH were used for further studies.

$$\text{Emulsion formation rate (\%)} = \frac{C_i - C_s}{C_i} * 100 \qquad (1)$$

$$\text{Coalescence rate (\%)} = 100 - \left(\frac{C_i - C_s}{C_i} * 100\right) \qquad (2)$$

where C_i and C_s (g) are the initial weight of oil taken and the weight of the separated amount of oil collected after mixing and resting, respectively.

2.5 Water salinity and the effect of temperature on the stabilization of oil droplets

Solutions with different salinities (0–4 g L^{-1}) were prepared for this study. Optimized concentration solutions were prepared using these solutions, to which oil was added keeping the oil/water ratio at 0.1. The remaining procedure of mixing and resting was performed as per section 2.4. The heights of the emulsified layer and coalescence layer were used to determine the oil droplets stabilization rate in the emulsion formed. Moreover, using optimized concentration and pH solution in DI and SW, the effect of temperature was studied at RT, 2 °C and -20 °C, respectively, with the same oil/water ratio. After mixing these solutions were rested at RT and 2 °C for one day. However, for -20 °C, the DI and SW with oil were stored in a deep freezer. After a day, these solutions were taken out and optimized concentration solution was added to them, mixed and stored back in the freezer. The oil droplet stabilization rate was studied periodically by measuring the oil droplet sizes with an optical microscope for 4 weeks. The oil droplets size was also measured with a laser diffraction spectrometer (Malvern Mastersizer 3000 with Hydro SV unit, UK).

2.6 Water quality after the emulsion stabilization and removal of oils

Traces of surface-active materials in water resources after the removal of oil are an important factor for the marine ecosystem after oil spill treatment. For this study, the top oil layer (either emulsified or

separate oil) was removed and the aqueous layer was tested using the NPOC method (TOC Analyzer, Shimadzu) in order to determine the amount of surface-active particles traces in the water.

3.0 Results and discussions

Carboxymethylated chitosan and hydrophobically modified carboxymethylated chitosan possess surface-active moieties such as carboxyl, hydroxyl and amino groups, and undergo a nucleophilic reaction to enhance their physiochemical properties. Similarly, OP-D also consists of surface-active functional groups such as hydroxyl and carboxyl. In CSOP-A, nucleophilic acyl substitution takes places between the free amino groups of the carboxymethylated polymer (Na-CMCS) and lauroyl chloride through an addition/elimination type mechanism. Furthermore, the hydroxyl groups of OP-D are also acylated with lauroyl chloride via similar substitution mechanism. There might be a cross-linking between the free amino groups of Na-CMCS and carboxyl groups of OP-D. Since the Blend is a mixture of hydrophobically modified carboxymethylated chitosan and OP-D, no further surface modification between them takes place, so these molecules either underwent intermolecular interaction or modified their own surfaces (see Figure 1) to enhance their existing physiochemical properties. The sizes of OP-D, CSOP-A and the Blend particles are shown in Figure S1 (refer Supplementary Material SM3).

3.1 Characterization

3.1.1 Surface Morphology

The surface morphology of the synthesized materials are shown in Figure 2 and Figure S1 (refer SM3). The surface of OP-D was clean and smooth (Figure 2a) whereas, in CSOP-A the formation of slits and clumps (see the white circled part of Figure 2b) suggests the mixed morphology of hydrophobic modification in chitosan derivative together with OP-D. However, in the Blend (Figure 2c), the slit formation was not so remarkable, as hydrophobically modified chitosan does not undergo further modification, except for mixing with OP-D. The EDS elemental composition (see Figures 2a-2c) shows the presence of sodium, revealing that CSOP-A and Blend are in sodium form, which was absent in OP-D. Even though there was the addition of hydrocarbon chain, the presence of sodium in these materials reduced their %C content in comparison to OP-D. The CHNS-O elemental results are shown in Table S2 of SM4. The BET surface area of OP-D, CSOP-A and Blend was 0.09 m^2/g, 0.39 m^2/g and 0.34 m^2/g, respectively. This shows that combining OP-D with chitosan derivatives enhances the surface structure of CSOP-A and Blend, so they were rougher and more porous than OP-D, which is in good agreement with the SEM results.

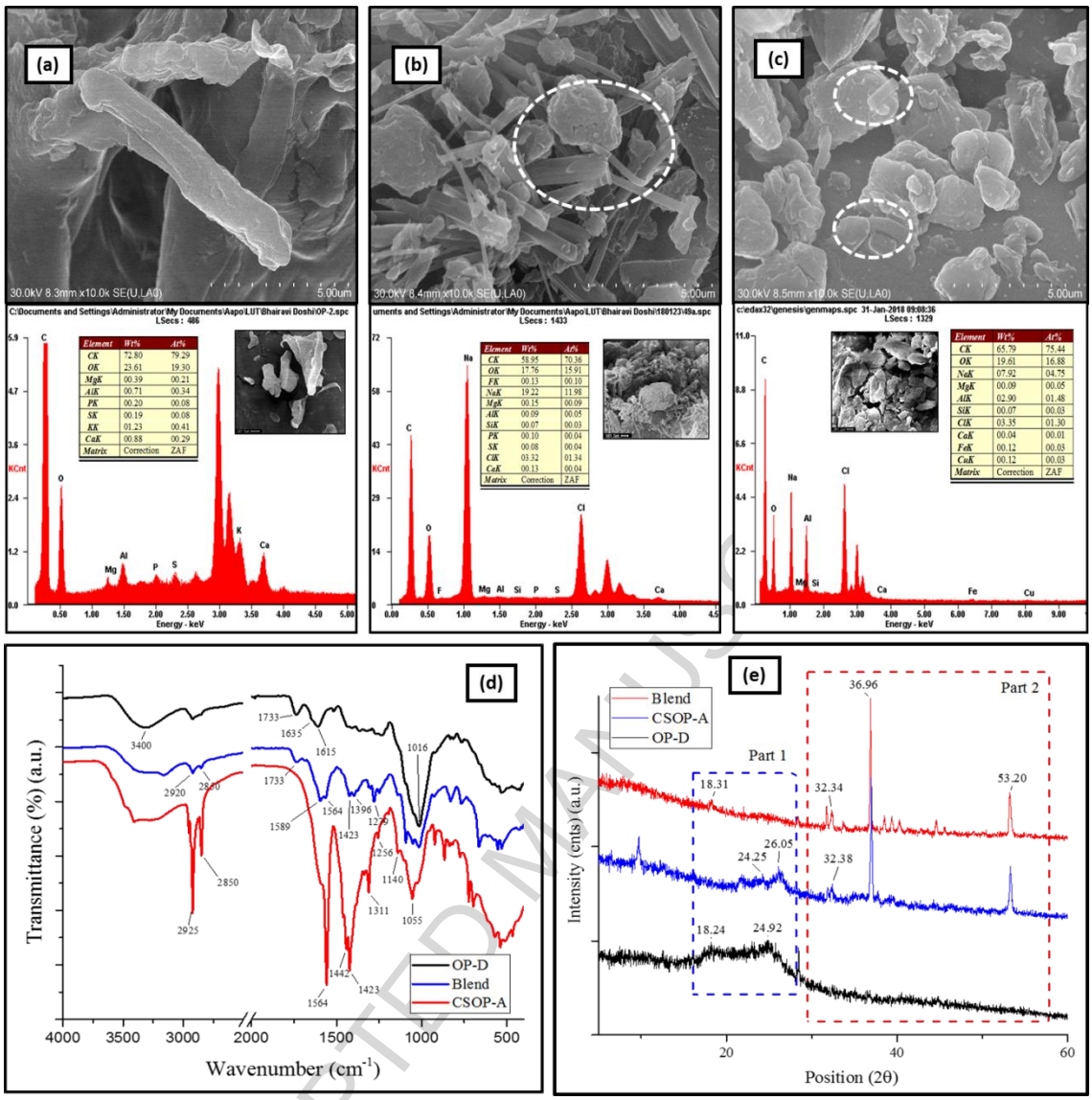

Figure 2: SEM Images and EDS results of (a) OP-D, (b) CSOP-A and (c) Blend along with FTIR spectra (d) and XRD spectra (e).

3.1.2 Spectrometric analysis

The FTIR spectra of OP-D, CSOP-A and Blend are shown in Figure 2d. In OP-D spectrum, the broad peak near 3400 cm^{-1} shows the –OH groups on pectin, cellulose, hemicellulose and lignin. 1733 cm^{-1} indicates C=O stretching, and 1615 cm^{-1} is attributed to C=C aromatic stretching, respectively. In addition, the peak at 1635 cm^{-1} is most likely the water peak. In CSOP-A, sharp peaks around 2925 cm^{-1} and 2850 cm^{-1} were attributed to the C-H stretching of lauroyl chains, 1564 cm^{-1} might be attributed to N-H (amide II) linkage revealing the incorporation of lauroyl moiety onto its surface after acylation [43]. Furthermore this peak might also be attributed to either imine (C=N) crosslinking between the sugar molecules of OP-D with the amino groups of chitosan through a Schiff base reaction [44] or

amide bond (=C-NH) between the carboxyl group of OP-D and amino groups of Na-CMCS [45]. The peaks at 1591 cm^{-1} and 1423 cm^{-1} are attributed to the C=O symmetric stretching of –COONa, respectively, so the 1733 cm^{-1} peak was absent in CSOP-A, as the carboxyl groups are in sodium salt form due to the alkaline pH during the synthesis. In the Blend, peaks at 2920 cm^{-1} and 2850 cm^{-1} show the C-H stretching of oleoyl chains, 1733 cm^{-1} indicates C=O stretching due to the presence of OP-D, and 1589 cm^{-1} indicates the –NH– group, respectively. The peak at 1016 cm^{-1} in OP-D and the Blend were attributed to the C-O group [46] [1]. Moreover, the peaks in the range of 850-1150 cm^{-1} were attributed to the C-O, C-C and C-O-C of the polysaccharide chain having a glycosidic bond and pyranoid ring [38] present in OP-D, CSOP-A and the Blend.

The XRD spectra are shown in Figure 2e. The XRD spectra of OP-D shows two peaks at 18° and 25°, but there were no other well-defined peak regions, which indicates the absence of a discrete mineral phase in OP-D. Thus, OP-D has a completely amorphous structure as expected for organic materials, and similar behaviour has also been previously observed [47]. The spectra of chitosan, Na-CMCS and NaO-CMCS are available in the supplementary data (Figure S2 in SM5). Compared to the XRD pattern of OP-D, the diffractogram of CSOP-A and the Blend showed sharper peaks indicating the formation of a new crystalline phase. The peak around 32° in CSOP-A and the Blend is attributed to the carboxymethylated part present in them, and similar results were previously observed for carboxymethylated chitosan [48]. In addition, the peaks around 37° and 53° (see part 2 of Figure 2e) were observed in CSOP-A and the Blend, might also be attributable to the acylation of carboxymethylated chitosan, which was absent in OP-D.

The ^{1}H NMR spectra are shown in Figure S3 of SM5. In the ^{1}H NMR spectrum of OP-D (Figure S3a of SM5), the signals at ~0.8–1.7 ppm originate from the fatty components and the signals at ~1.9–2.2 ppm show the presence of O-linked acetate [49]. The spectral region of 3.0–6.0 ppm is associated with ring hydrogen and mainly the presence of sucrose, fructose and glucose, as witnessed by their respective intensities and previous literature results [50,51]. However, in the CSOP-A spectrum (Figure S3b of SM5), the reduction of peak intensities in this region compared to OP-D reflects that the –OH groups of sugars moieties present in OP-D might have been substituted during acylation. Moreover, in the CSOP-A spectrum, the peaks in the range of 1.1–2.0 ppm are attributed to the alkyl (CH_2 and CH_3) group of the lauroyl chain. The signal obtained at 2.0 ppm corresponds to –NH-CH– linkage, obtained through linkage of the –C=O– group of carbohydrate or pectin in OP-D with the $–NH_2$ group of chitosan derivative [52], and also attributed to the CH_2 groups of the lauroyl chain. The new peak near 8.1 ppm is

attributed to the imine bond for the linkage between $–NH_2$ group of chitosan derivative and the –C=O– group of OP-D. This is in agreement with the FTIR results. The peak resonance in the Blend (Figure S3c of SM5) and CSOP-A near to 3.7 and 4.1–4.6 ppm is attributed to carboxymethyl protons such as N-CH_2-CO- and O-CH_2-CO-, respectively. Moreover, the signals at ~0.8–1.7 ppm in the Blend originate from the alkane proton of oleoyl chain as well as fatty components present in OP-D.

3.1.3 Surface charge of OP-D, CSOP-A and Blend with different water quality, interfacial tension (IFT) and wettability

The initial pHs of OP-D, CSOP-A and the Blend in DI were 5.5, 9.5 and 7.4, respectively. The magnitude of the surface charge depends on the acidic or basic strengths of the surface groups and on the pH of the solution. In OP-D, when pH is increased, deprotonation of the carboxyl group occurs, which then results in a decrease in zeta potential value (i.e. more negative zeta potential). On the other hand, when pH decreases, carboxyl groups are associated (i.e. protonated), which results in neutralization of charge and a consequent increase in zeta potential (see Figure 3a). The ZP below pH 4 and above 10 were not considered due to the dissolution of OP-D components. In case of CSOP-A and the Blend, simultaneous protonation of carboxyl and amino groups occurred with a decrease in pH, which increased the ZP overall by neutralizing the charge (see Figures 3b-3c). Another reason might be the competing interactions between the oppositely charged amino groups and carboxyl groups to neutralize the surface charge, and similar behaviour has been previously observed [11]. So, when pH is decreased to 4, the surface charge in CSOP-A seems to be close to zero (i.e. no surface charge). In hypothesis, the hydrophobic segments in CSOP-A and the Blend affects the conformations of polymers, as they disturb the aggregation and formations of particles, and thus the ZP (see Figure S4 of SM6 for the phase diagram). Furthermore, the carboxymethylated groups in the Blend and CSOP-A are attributable to a more negative surface than OP-D. As shown in Figures 3a-3c, the ZP were less negative in SW than in DI. One reason might be that the ions present in SW formed an electrical double layer with the surface charges of these materials. Furthermore, there might be ion exchange between the surface charge and electrolyte with decreasing pH (see SM6 for conductivity). In figure 3d, the hump near pH 6.5 shows the protonation of amino groups in the Blend and CSOP-A, which was absent in OP-D. The protonation rate in CSOP-A was less than the Blend, which suggests that some amino groups might have linked with OP-D, instead of linking with lauroyl moieties during acylation. This is in a good agreement with FTIR and NMR interpretations.

IFT is the prime parameter for the formation of emulsion and its stability. The surface-active agents, by orienting their hydrophilic groups towards the aqueous phase and hydrophobic groups towards the oil phase, reduce the IFT between these two phases. The initial IFT between marine diesel and the water phase (deionized water and saline water) without any OP-D, CSOP-A and the Blend was 15.55 ± 0.08 mN/m and 34.76 ± 0.68 mN/m, respectively. A small addition of OP-D, CSOP-A and the Blend in DI reduces the IFT by sequential, whereas with SW this reduction was drastic (refer Figures 3e-3f). This shows that the presence of hydrophobic moieties made CSOP-A and the Blend more amphiphilic, which drastically reduced the IFT. Generally, the lower the IFT, the higher the emulsion stability. The wettability of the particles was determined by contact angle using the sessile drop method. The contact angle of OP-D, Blend and CSOP-A were about 63°, 83° and 113°, respectively (see Figure S6 of SM6). This shows that hydrophobic moieties in the Blend and CSOP-A enhanced the contact angle as compared to OP-D. Kaptay also suggested that the optimum contact angle for the stabilization of emulsions by a single or double layer of particles is <90° or <129°, for o/w emulsion [53]. Furthermore, the polar and non-polar parts of these materials show "like-dissolves-like" characteristics, i.e. the polar part will show the dissolution in the aqueous phase and non-polar in the oil phase.

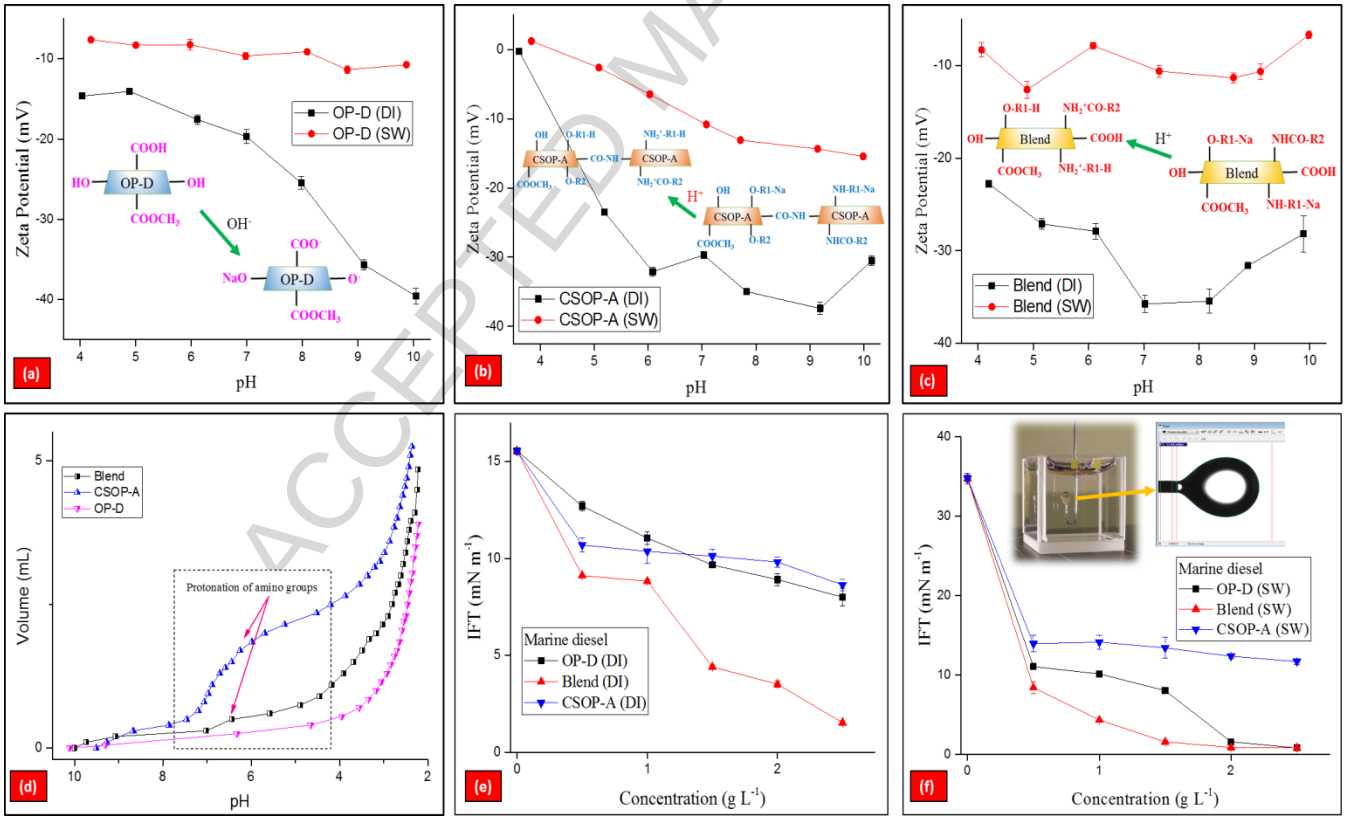

Figure 3: Zeta potential of OP-D (a), CSOP-A (b) and the Blend (c) in deionized water (DI) and saline water (SW) at different pH levels. Potentiometric titration curve of OP-D, CSOP-A and the Blend (d).

Interfacial tension (IFT) between marine diesel and the water phase (e) deionized water and (f) saline water in the presence of OP-D, CSOP-A and the Blend using the pendant drop method.

3.2 Emulsion formation as a function of OP-D, CSOP-A and Blend dosage

The behaviour of the surface-active particles mainly depends on water quality and type of oil, and IFT and wettability determine emulsion efficacy. Figure 4a shows the emulsion formation rate of marine diesel versus surface-active particles dosage at native pH. The increase in OP-D concentration in DI increased the emulsion formation rate from 5% to 70%. This suggests the adsorption of OP-D at the interface, which resists droplet coalescence via electrosteric stabilization. On other hand, OP-D particles being smaller in size provides a barrier against droplets coalescence (Figure 4b1), resulting in solid-stabilized (Pickering) emulsion. The presence of hydrophobic hydrocarbon segments in the Blend reduces the IFT as compared to OP-D (refer Figure 3e), so the effectiveness of the Blend was more than 80% even with a low dosage (0.5 g L^{-1}). This reveals that the orientation of the hydrophobic hydrocarbon segments (oleoyl groups) of the Blend at the oil-water interface have generated a steric barrier between the oil droplets. Furthermore, the magnitude of this steric barrier between the droplets was enhanced with the increasing concentration of the Blend, due to the dense packing and thick interface of the molecules around the oil droplets (Figure 4b2). In addition, there is also formation of the Pickering emulsion in the Blend due to presence of OP-D. This resulted in an overall increase in the emulsion formation rate. Despite the hydrophobic moieties in CSOP-A, the maximum stabilisation rate was about 50%, which might be because of the exposure of the non-polar region to the surrounding water, which has started generating hydrophobic attraction between the droplets [54] due to the rupturing of the steric interactions of CSOP-A from the oil droplets. This resulted in the aggregation of oil droplets and destabilization of the emulsion (Figure 4b3). Although CSOP-A and the Blend have a negative surface ZP in DI (Refer Figures 3b-3c), the emulsion formation rate varied in them due to the presence of different hydrocarbon segments. Shiao et al. previously demonstrated the effect of the hydrocarbon chain on oil stabilization [55]. In addition, lengthening the hydrocarbon chain also enhanced ions exchange and hydrophobic interactions [56,57], so the interaction of CSOP-A with marine diesel differs from the Blend. Furthermore, the o/w emulsion behavior was gel-like in the Blend due to the presence of OP-D whereas, with CSOP-A, creamy emulsions were observed (Figure 4b). The oil droplet size in OP-D (Figure 4c) and the Blend (Figure 4d) was thus >100 µm, whereas it was <100 µm in CSOP-A (Figure 4e). The coalescence rate dominated the droplets stabilization rate with CSOP-A in SW, whereas the presence of OP-D in the Blend showed more than 90% conversion of oil into emulsion, even at a very small dosage (refer Figure S7 of SM7 for emulsion formation). Our previous

results demonstrated that a dosage of about 2.0 g L^{-1} NaO-CMCS was required to form stable emulsion with SW [43]. On the other hand, this study shows that the addition of OP-D to NaO-CMCS reduces the dosage to half with the same SW. This shows that water salinity decreases the critical micelle concentration of the Blend. Similar results have been previously observed [58].

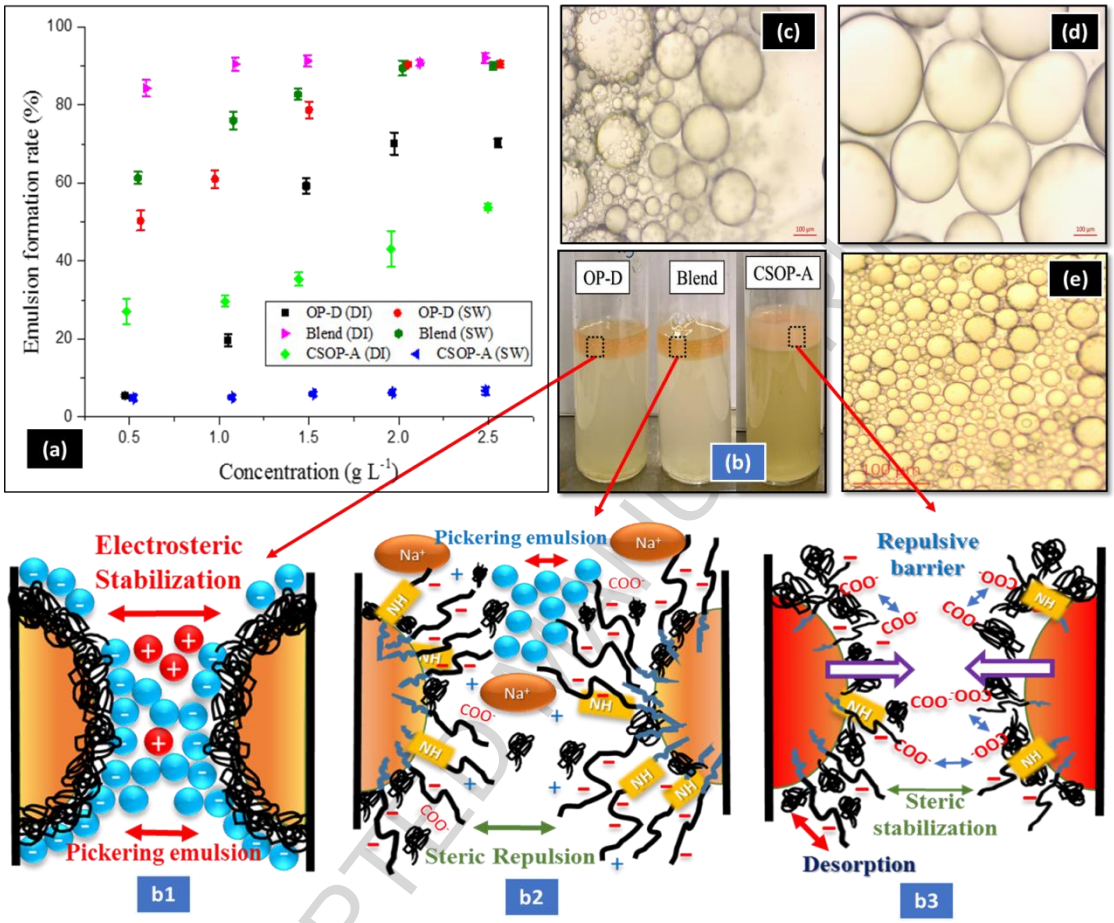

Figure 4: (a) Effect of OP-D, CSOP-A and the Blend dosage in the emulsion formation of marine diesel, (b) emulsion formation with marine diesel having 2.0 g L^{-1} of dosage OP-D, CSOP-A and the Blend in DI along with the emulsion mechanism with OP-D (b1), the Blend (b2) and CSOP-A (b3). Microscopic images of o/w emulsion for (c) OP-D (d) the Blend and (e) CSOP-A with marine diesel in DI taken at a magnification of 100 µm.

The emulsion formation 2T-oil (Refer figure 5a) differs from marine diesel in its composition. 2T-oil, being viscous, consists of solvent-dewaxed heavy paraffinic and polyaromatics, that can easily form a creamy layer with water even in the absence of oil emulsifier/surface-active particles. Furthermore, a small addition of either OP-D, the Blend or CSOP-A converts this creamy layer to an emulsified layer (Figures 5b and S8). However, the droplet stabilization rate is more likely to be dependent on the type of water for CSOP-A as, with DI, this rate was about 22%, whereas with SW it was about 90%. This also

shows that the presence of different hydrocarbon chains in CSOP-A might have affected the emulsion stability and behaviour as discussed earlier but, for the remaining materials, the droplet stabilization rate (emulsion formation) was more than 80% with DI and SW. Although the emulsion behaviours were not identical, the oil droplet sizes in the emulsions were <100 µm (Figures 5c-e), so the optimal dosage of these materials was 2.0 g L^{-1} for all further studies.

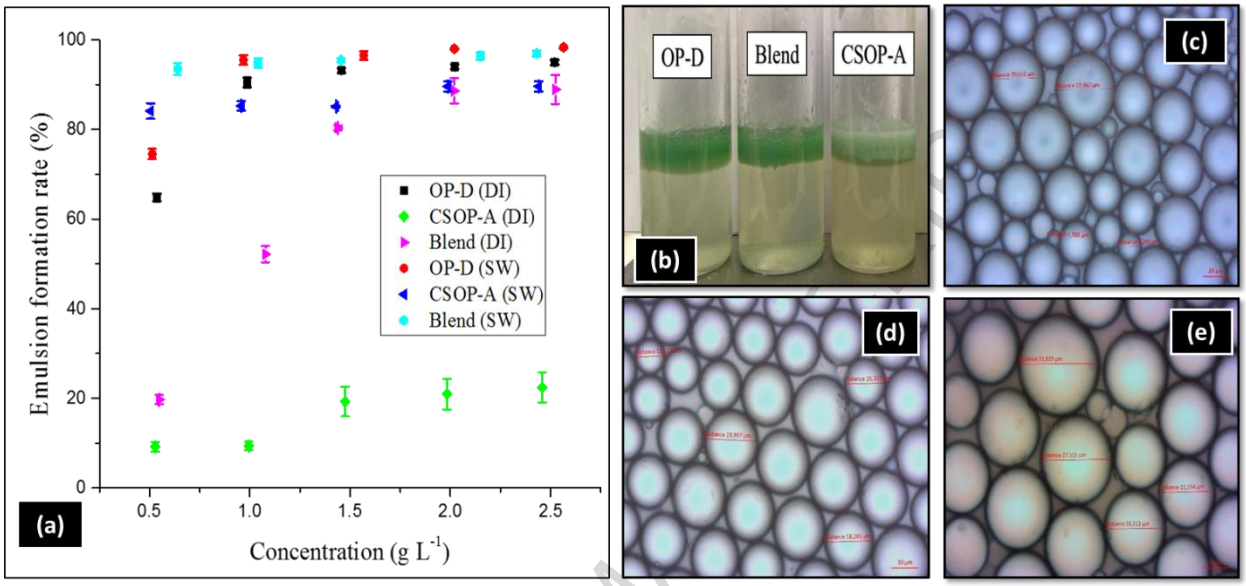

Figure 5: (a) Effect of OP-D, CSOP-A and the Blend dosage in the emulsion formation of 2T-oil, (b) the o/w emulsion with 2T-oil with 1.5 g L^{-1} of dosage OP-D, CSOP-A and the Blend in SW, microscopic images of o/w emulsion for (c) OP-D (d) the Blend and (e) CSOP-A with 2T-oil in SW taken at a magnification of 10 µm.

3.3 Emulsification behavior of oils with OP-D, CSOP-A and the Blend at different pH levels

The pH of wastewater-containing oil or spilled oil plays a significant role in the applicability of the surface-active materials. When OP-D interacted with marine diesel at its initial pH (5.5), there was a formation of gel-like emulsion suggesting the bridging of particles between droplets and particle-particle interaction. So the obtained emulsion is either Pickering emulsion or can be attributed to the hydrogen bonding and to bonds between hydrophobic groups and oil droplets via steric barriers [59]. In addition to steric stabilization, the electrostatic contribution to this stabilization is quantified by electrophoretic mobility (EM) proportional to the surface charge. The EM value of OP-D at pH 4 is -1.14 µmcm/Vs, and decreases to -3.10 with increasing pH (Figure 6a). This shows the dissociation of carboxyl groups present in OP-D at a lower pH, which forms a thicker adsorbed gel-like layer with oil via electrosteric barriers whereas, at higher pH, the lower value of EM tends to form o/w emulsion mainly due to steric stabilization or Pickering emulsion. The electrolyte in SW increases the EM (Figure

6b) compared to OP-D in DI water, by shielding the negative charges and enhancing the emulsion rate [60] through the electrostatic barriers of electrical charges. The overall obtained emulsion was therefore due to steric and electrostatic stabilization. However, the OP-D solution contains some non-dispersible parts, which form sediments and do not take part in the formation of an emulsion (Figure 6c).

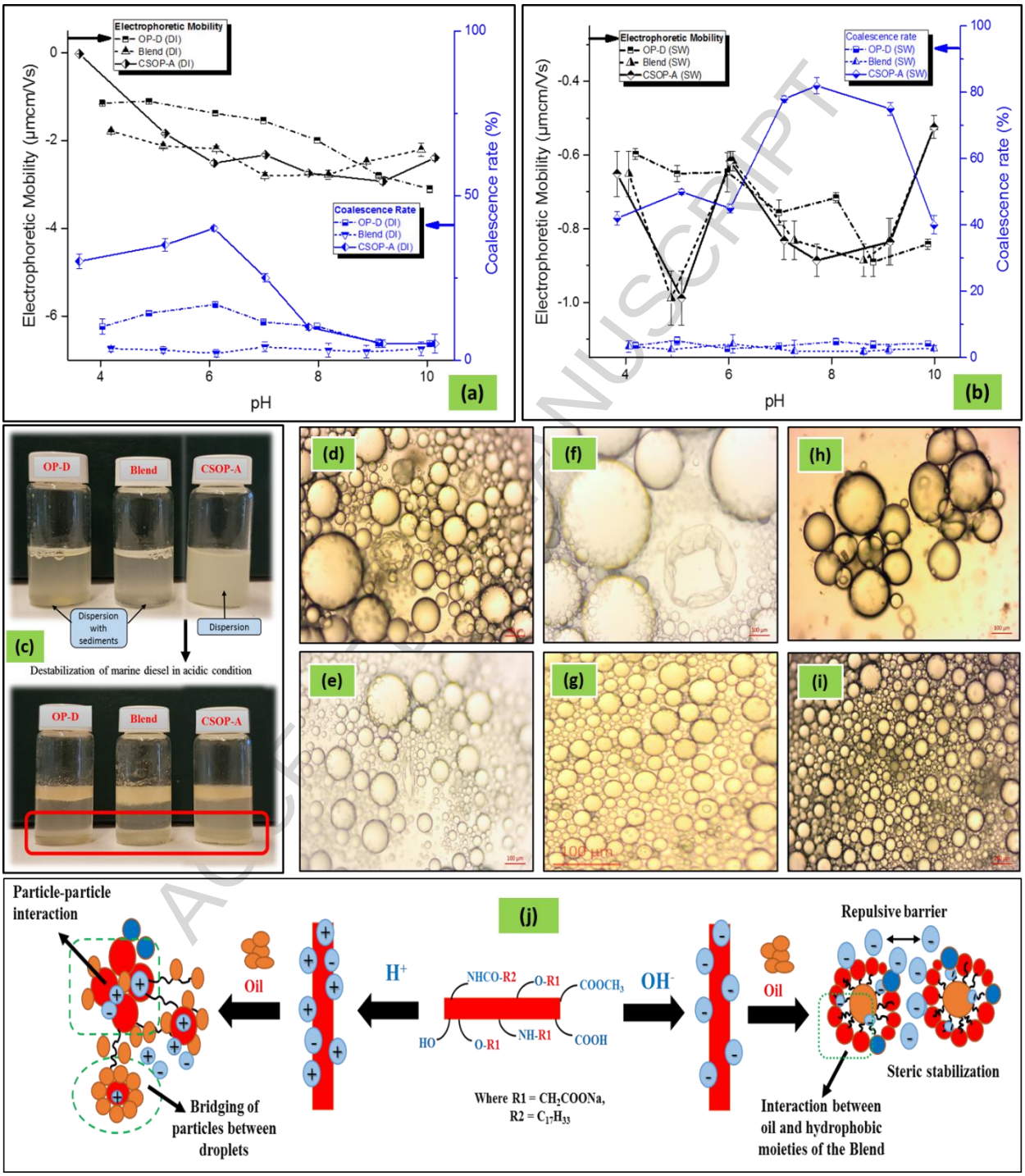

Figure 6: Effect of solution pH of OP-D, CSOP-A and the Blend on the electrophoretic mobility and coalescence rate of marine diesel (a) with deionized water and (b) with saline water. Electrophoretic

mobility is shown with black lines with symbols and coalescence rate is shown with blue lines with symbols. (c) The emulsion formation of marine diesel with OP-D, CSOP-A and the Blend in acidic condition. Microscopic images of the o/w emulsion of marine diesel in DI water with OP-D at (d) acidic pH 4.1 and (e) alkaline pH 9.9, with CSOP-A at (f) acidic and (g) alkaline pH, with the Blend at (h) acidic and (i) alkaline pH, at a magnification of 100 µm. (d) Emulsion mechanism of marine diesel with 2.0 g L^{-1} of Blend in DI at acidic and alkaline pH.

The microscopic images of o/w emulsion at different pH levels in DI and SW are shown in Figures 6d-6i and Figure S9 of SM8, respectively. Since CSOP-A possessed a glucosamine backbone along with OP-D, the EM values differ from OP-D at a different pH range, so the oil stabilization differs. In addition, the increment of EM values from the alkaline to acidic pH region implied the adsorption of surface-active particles via hydrophobic bonding, distributed on the external surfaces of aggregates. Although there were long hydrocarbon segments in CSOP-A, the simultaneous protonation of amino and carboxyl groups occurred in CSOP-A with decreasing pH and mitigated the oil droplets' resistance to coalescence by stepping down the emulsion rate (Refer Figures 6f-6g for the microscopic images). For the Blend, pH did not have a significant effect on the droplet stabilization rate, but rather changed the nature of the o/w emulsion, i.e. gel-like emulsion at acidic pH and creamy emulsion at alkaline pH (refer Figures 6h-6i for the microscopic images and Figures 6j along with its mechanism). In addition, emulsion formation with the Blend was independent of water quality, as some of the hydrophobically modified chitosan in the Blend was effective in DI and some of OP-D present in the Blend was effective with SW.

The droplets stabilization rate of 2T-oil in DI was more dependent on pH, than that in SW (Figure S10 in SM8), since the cation exchange from SW with H^+ of surface-active moieties (−COOH and –OH) of OP-D and the Blend formed bulky o/w emulsion. In addition, the IFT of 2T-oil is less in SW than DI, which resulted in the dissolution of some compounds of 2T-oil in SW, and a similar result was previously reported [61]. Furthermore, 2T-oil swells easily in SW, resulting in spontaneous oil-in-water emulsification, which diffuses the surfactants across the interface and forms bulky emulsion [62]. Nevertheless, for OP-D and the Blend, decreasing pH formed an interfacial monolayer that contributed to the prevention of dispersed 2T-oil droplets to coalescence, resulting in a creamy and gel-like emulsion. Even though the EM values of the Blend and CSOP-A do not differ much in SW with changing pH, the emulsion behaviour changes in them due to the presence of OP-D and crosslinked OP-D. Although the Blend and CSOP-A possess long hydrocarbon chains, the pH gradient at the interface

affects the steric barriers and prevents the adsorption of long chains towards 2T-oil, which might have increased the coalescence rate. Moreover, the protonation of amino groups in the CSOP-A with decreasing pH provides repulsive barriers, which slightly resist the aggregation of droplets, so the coalescence rates of these hydrophobically modified materials varied in DI.

3.4 The role of water salinity in the stabilization rate of oil droplets

Different surface-active particles and their oil droplets stabilization capacity with respect to the salinity of water are equally as important as pH. Figure 7a shows the oil droplet stabilization of marine diesel in the formed emulsion as a function of salinity. With OP-D, the droplet stabilization rate of marine diesel increased with increasing electrolyte concentration, whereas the orange-chitosan derivatives indicated droplet stabilization in a different way. One of the reasons might be that the presence of electrolyte prevents hydration water around OP-D molecules that reduces the electrostatic repulsion between the intermolecular hydrophilic groups, and enhances the hydrophobicity of OP-D. Similar behaviour of surfactant was previously observed [58]. Furthermore, the crosslinking of metal ions with carboxyl and hydroxyl groups present in OP-D might have reduced intermolecular electrostatic repulsion. Kasprzak et al. demonstrated the coordination of metal ions with flavonoids to form complexes [63]. In CSOP-A, the unavailability of carboxylic acid reduced crosslinking activity with ions, and thus reduced its effectiveness in the emulsion stability at SW salinity. Although CSOP-A possesses hydrocarbon chains, an increase in electrolyte concentration strengthened the electrostatic interaction of unreacted hydroxyl groups towards water, which enhanced the aggregation of oil droplets and destabilized the emulsion of marine diesel. In case of the Blend, the stabilization rate was not affected much with salinity variance in DI, due to the steric forces.

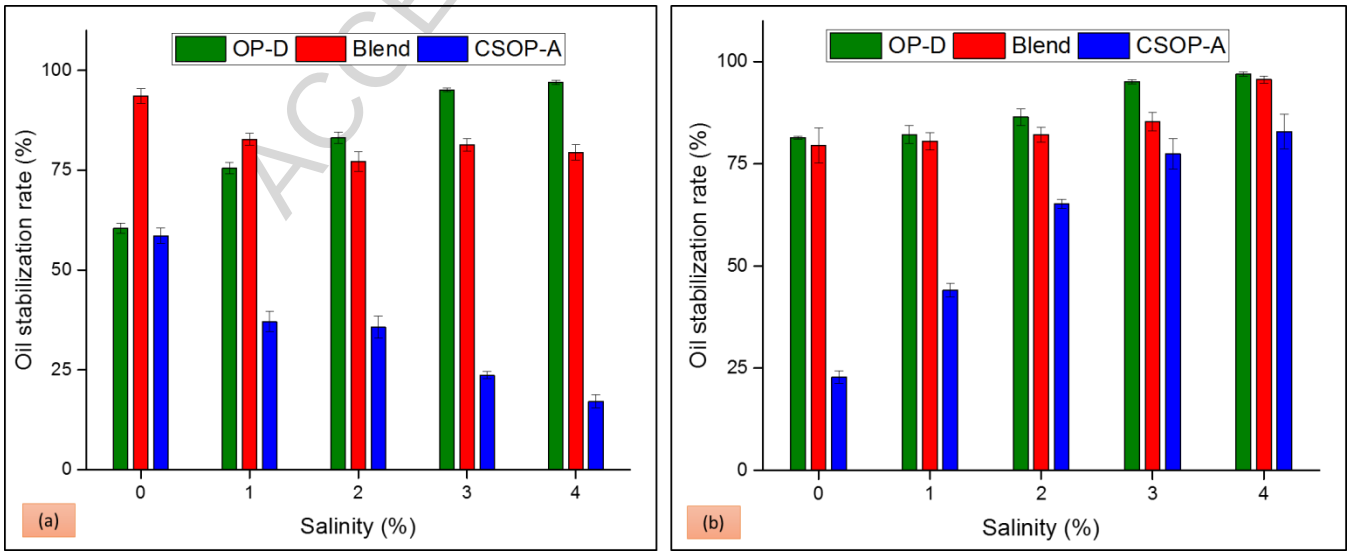

Figure 7: Effect of salinity on the stabilization of oil droplets in the formed emulsion (a) Marine diesel and (b) Marine 2T oil using OP-D, CSOP-A and the Blend.

2T-oil consists of solvent-dewaxed heavy paraffinic and polyaromatics along with hydrocarbons, which immediately form clusters when mixed with SW. Even though the oil droplets stabilization rate is similar (Figure 7b), the nature of emulsion with respect to these materials was different. OP-D formed stable emulsion that could be skimmed easily, whereas CSOP-A and the Blend formed bulky lumps due to the long hydrocarbon chain present in these derivatives. Secondly, the presence of electrolyte led to stronger interfacial activity with these surface-active species, by limiting the coalescence effect and then the stabilization [64].

3.5 Behaviour of oil droplets in the formed emulsion with changing temperature

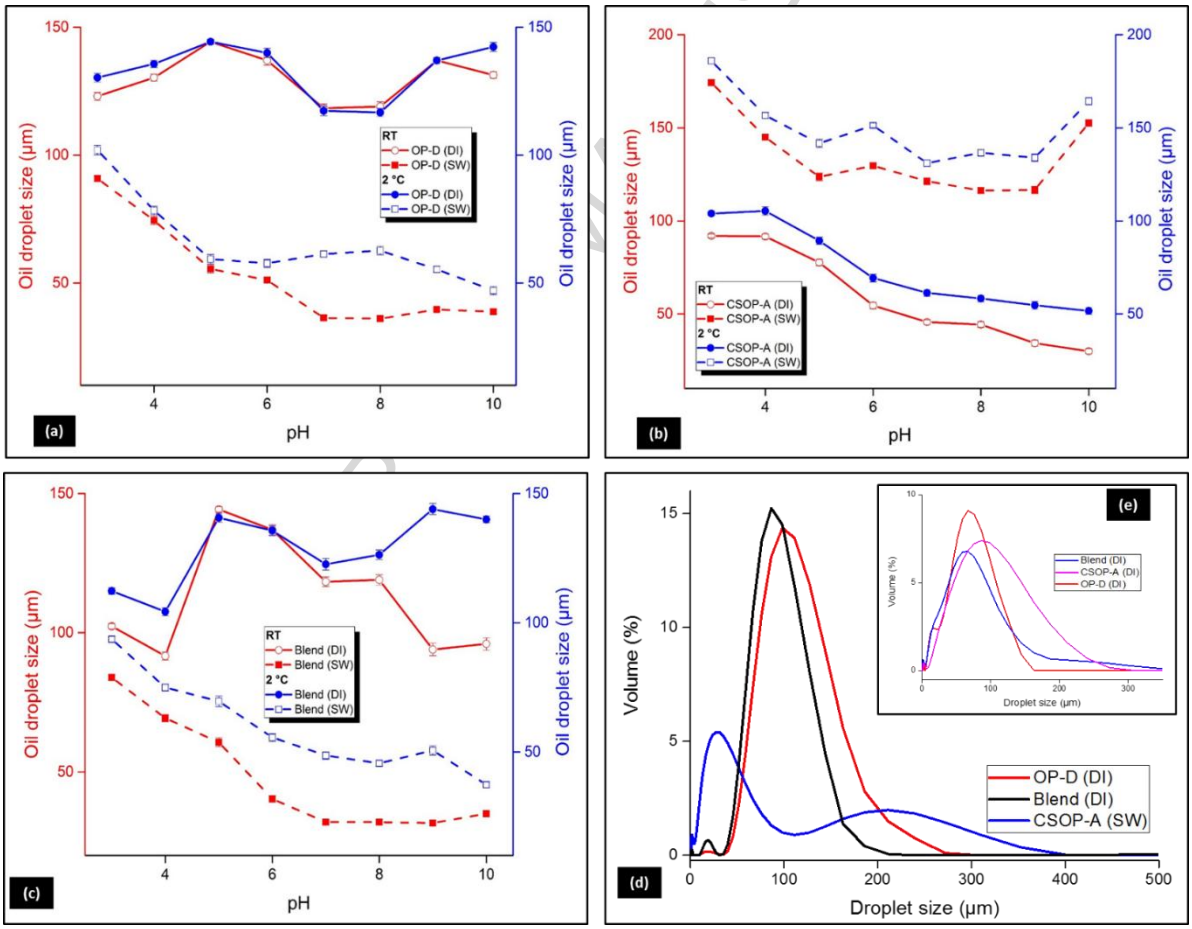

Figure 8: Oil droplet size in the o/w emulsion at RT and 2°C for marine diesel using (a) OP-D, (b) CSOP-A and (c) Blend using optical microscope. The droplet size measured with a laser diffraction spectrometer of (d) marine diesel with optimized dosage, i.e. 2.0 g $L^{-1}$of OP-D, CSOP-A and the Blend with a different quality of water at RT and (e) 2T-oil with the same dosage in DI.

The measured oil droplet sizes in the o/w emulsion in varying pH at RT and 2°C for marine diesel using optical microscope are shown in figures 8(a-c). The emulsion rate of the oils at RT and 2°C does not fluctuate much apart from the size of oil droplets in the emulsion. In addition, the water quality also affected the oil droplet size. The droplet size of marine diesel fluctuates with different surface-active particles used at RT (figure 8d). In the case of 2T-oil, the oil droplet size in the emulsion was less than 100 µm (figure 8e), but at -20°C due to the ice formation, the water quality did not play a significant role in the formation of o/w emulsion due to the ice, but was rather more dependent on surface-active materials concentration. Therefore, the oil droplets stabilization rate (emulsion formation) on the surface of ice in the presence of these surface-active materials decreased to less than 10%. Despite hydrophobic moieties in CSOP-A and the Blend, the absence of the liquid-dispersed phase suppressed the hydrophilic properties of these surfactants, which in turn inhibited the formation of emulsion. Secondly, in such cold conditions, the viscosity of the oils increases, which might be one reason for the ineffectiveness of these materials in the formation of emulsion. These particle-formed surfactants were effective for spilled oil above 0°C, due to their dispersion in water, but below 0°C there was a decline in the dispersion rate and particle effectiveness in the stabilization of oil droplets or formation of the emulsion also declined.

3.6 Water quality after the removal of oil

The remains of toxic chemical dispersants in water resources after the removal of spilled oil adversely affects marine creatures, due to their poor biodegradability, so to investigate the amount of dispersant traces in water is equally as important as the removal of spilled oil. Traces of organic matter after the removal of emulsified/separated oil were investigated using TOC through the NPOC method. The aqueous layer was not cleared (see Figures 4b, 5b and 6c), indicating traces of unreacted surface-active particles. Figures 9a and 9b shows the traces of OP-D, the Blend and CSOP-A after the removal of the oil/emulsified marine diesel and the 2T-oil layer. Despite the removal of the oil layer, the increase in the amount of organic carbon was attributed to either the adsorption of oil molecules on the surface-active moieties or the presence of degraded oil in the continuous aqueous phase along with these particles. Especially for 2T-oil, the spontaneous oil-in-water emulsification implies the leaching of surfactant from oil to the aqueous phase [62]. However, the amount of increased TOC after 2T-removal was less (Figures 9c-d) than that obtained from marine diesel due to the formation of bulky emulsion, in which the surface-active particles might have become trapped. Various biosurfactants derived from varied microbial sources are present in the water, enhancing the biodegradation of the dispersed crude oil through bioremediation [65]. Moreover, earlier studies demonstrate orange peel as a substrate for

Bacillus Licheniformis biosurfactant production and the biodegradation of hydrocarbons [66], so traces of OP-D in the water phase proved to be non-toxic. Chitosan being non-toxic and biodegradable, its derivatives, the Blend and CSOP-A, might not have many adverse effects, if found in water resources.

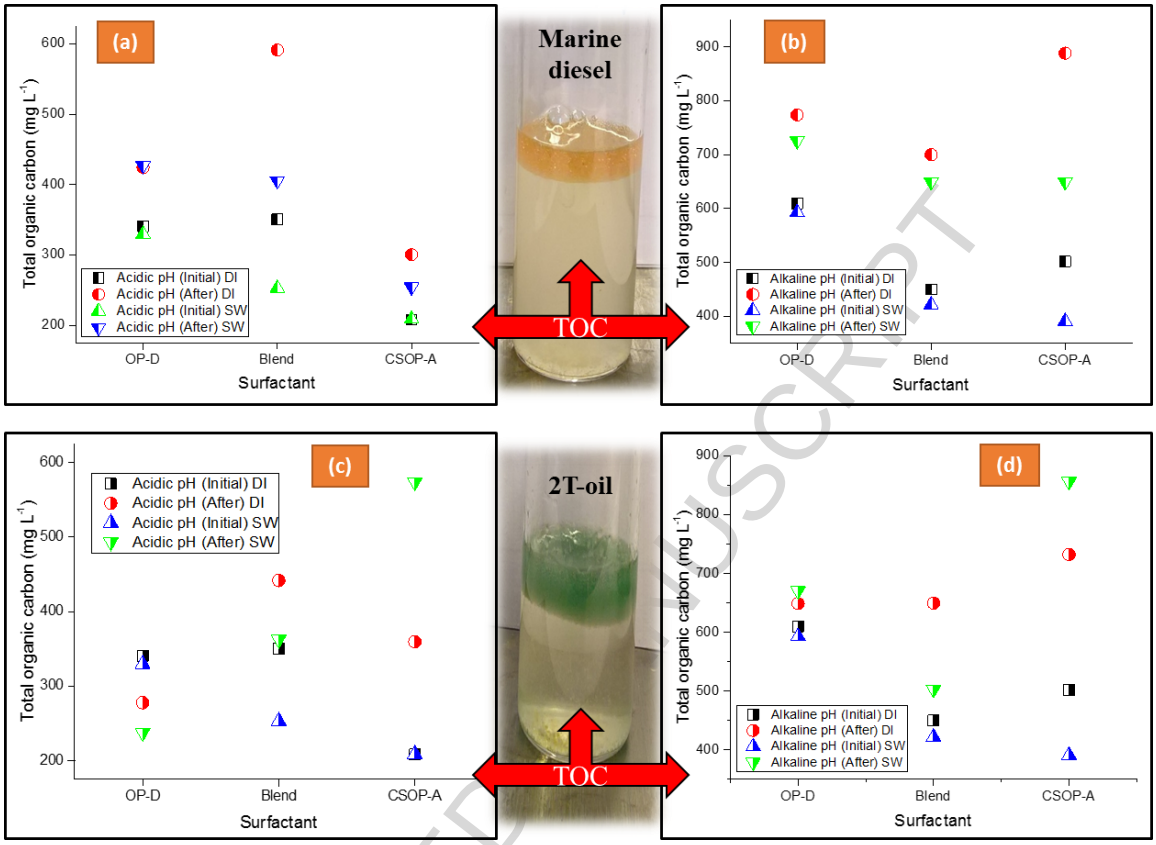

Figure 9: Total organic carbon (TOC) content after the removal of marine diesel (a) at acidic pH and (b) at alkaline pH, and after the removal of 2T-oil (c) at acidic pH and (d) at alkaline pH from the water surface.

4.0 Conclusions

The use of bio-waste such as orange peel together with chitosan derivatives facilitate oil droplet breakup through faster adsorption of their surface-active moieties at the oil-water interface. The spectrometric measurements confirmed hydrophobic modification along with the presence of surface-active moieties on the surface of OP-D, CSOP-A and the Blend. The emulsion formation rate of marine diesel followed the order of the Blend > OP-D > CSOP-A, whereas for 2T-oil the order was OP-D > Blend > CSOP-A. The emulsion formation was solid-stabilized (Pickering) emulsion with OP-D, a combination of Pickering and conventional o/w emulsion with the Blend and only conventional emulsion with CSOP-A. The emulsion formation rate was more than 90% with OP-D in saline water, whereas, the Blend balanced the same rate independent of the water quality with optimized concentration. For CSOP-A, the

droplets stabilization rate in the formed emulsion was more dependent on water quality and oil. This revealed that different hydrophobic moieties on the surface of the Blend and CSOP-A affected the oil droplets stabilization rate. The presence of glucosamine unit and carboxymethyl moieties in the Blend and CSOP-A altered the nature of emulsion with changing pH. There was a direct influence by temperature on the oil-droplet formation and its stability. The emulsion formed at RT was most stable, and at -20 °C this rate decreased to 10%, but the stabilization rate was not affected much at 2°C except the increase in droplet size, so the studied surface-active particles could be used in dispersant formulation even at Arctic temperatures. Since the origin of these materials is bio-based, their hazardousness could be less than materials used in commercial dispersants. The future need is to identify different types of bio-waste and reutilize them as dispersants in oil spill response and accordingly minimize the use of hazardous chemicals.

Note

The authors declare no competing financial interest.

Acknowledgement

The authors are grateful to the Academy of Finland (decision number 283200) for funding this project.

References:

[1] R.T. Ranellone, P. Tukaew, X. Shi, A.S. Rangwala, Ignitability of crude oil and its oil-in-water products at arctic temperature, Mar. Pollut. Bull. 115 (2017) 261–265. doi:10.1016/j.marpolbul.2016.12.021.

[2] L. van Gelderen, J. Fritt-Rasmussen, G. Jomaas, Effectiveness of a chemical herder in association with in-situ burning of oil spills in ice-infested water, Mar. Pollut. Bull. 115 (2017) 345–351. doi:10.1016/j.marpolbul.2016.12.036.

[3] S.M. Beladi-Mousavi, B. Khezri, L. Krejčová, Z. Heger, Z. Sofer, A.C. Fisher, M. Pumera, Recoverable Bismuth-Based Microrobots: Capture, Transport, and On-Demand Release of Heavy Metals and an Anticancer Drug in Confined Spaces, ACS Appl. Mater. Interfaces. 11 (2019) 13359–13369. doi:10.1021/acsami.8b19408.

[4] C.F. Wise, J.T.F. Wise, S.S. Wise, W.D. Thompson, J.P. Wise, J.P. Wise, Chemical dispersants used in the Gulf of Mexico oil crisis are cytotoxic and genotoxic to sperm whale skin cells, Aquat. Toxicol. 152 (2014) 335–340. doi:10.1016/j.aquatox.2014.04.020.

[5] M. Zheng, M. Ahuja, D. Bhattacharya, T.P. Clement, J.S. Hayworth, M. Dhanasekaran, Evaluation of differential cytotoxic effects of the oil spill dispersant Corexit 9500, Life Sci. 95 (2014) 108–117. doi:10.1016/j.lfs.2013.12.010.

[6] J.C. Athas, K. Jun, C. McCafferty, O. Owoseni, V.T. John, S.R. Raghavan, An Effective Dispersant for Oil Spills Based on Food-Grade Amphiphiles, Langmuir. 30 (2014) 9285–9294. doi:10.1021/la502312n.

[7] D.A. Riehm, J.E. Neilsen, G.D. Bothun, V.T. John, S.R. Raghavan, A. V. McCormick, Efficient dispersion of crude oil by blends of food-grade surfactants: Toward greener oil-spill treatments,

Mar. Pollut. Bull. 101 (2015) 92–97. doi:10.1016/j.marpolbul.2015.11.012.
[8] X. Wu, L. Zhang, X. Zhang, Y. Zhu, Y. Wu, Y. Li, B. Li, S. Liu, J. Zhao, Z. Ma, Ethyl cellulose nanodispersions as stabilizers for oil in water Pickering emulsions, Sci. Rep. 7 (2017) 12079. doi:10.1038/s41598-017-12386-4.
[9] J. Ojala, J.A. Sirviö, H. Liimatainen, Nanoparticle emulsifiers based on bifunctionalized cellulose nanocrystals as marine diesel oil–water emulsion stabilizers, Chem. Eng. J. 288 (2016) 312–320. doi:10.1016/j.cej.2015.10.113.
[10] B. Doshi, E. Repo, J.P. Heiskanen, J.A. Sirviö, M. Sillanpää, Effectiveness of N,O-carboxymethyl chitosan on destabilization of Marine Diesel, Diesel and Marine-2T oil for oil spill treatment, Carbohydr. Polym. 167 (2017) 326–336. doi:10.1016/j.carbpol.2017.03.064.
[11] S. Kalliola, E. Repo, V. Srivastava, F. Zhao, J.P. Heiskanen, J.A. Sirviö, H. Liimatainen, M. Sillanpää, Carboxymethyl Chitosan and Its Hydrophobically Modified Derivative as pH-Switchable Emulsifiers, Langmuir. 34 (2018) 2800–2806. doi:10.1021/acs.langmuir.7b03959.
[12] G. Pi, Y. Li, M. Bao, L. Mao, H. Gong, Z. Wang, Novel and Environmentally Friendly Oil Spill Dispersant Based on the Synergy of Biopolymer Xanthan Gum and Silica Nanoparticles, ACS Sustain. Chem. Eng. 4 (2016) 3095–3102. doi:10.1021/acssuschemeng.6b00063.
[13] K. Kurita, Chitin and Chitosan: Functional Biopolymers from Marine Crustaceans, Mar. Biotechnol. 8 (2006) 203–226. doi:10.1007/s10126-005-0097-5.
[14] M. Rinaudo, Chitin and chitosan: Properties and applications, Prog. Polym. Sci. 31 (2006) 603–632. doi:10.1016/j.progpolymsci.2006.06.001.
[15] FAO, The state of World Fisheries and Aquaculture 2106. Contributing to food security and nutrition for all, 2016. doi:92-5-105177-1.
[16] N. Yan, X. Chen, Sustainability: Don't waste seafood waste, Nature. 524 (2015) 155–157. doi:10.1038/524155a.
[17] B. Doshi, M. Sillanpää, S. Kalliola, A review of bio-based materials for oil spill treatment, Water Res. 135 (2018) 262–277. doi:10.1016/j.watres.2018.02.034.
[18] R.R. Fouad, H.A. Aljohani, K.R. Shoueir, Biocompatible poly(vinyl alcohol) nanoparticle-based binary blends for oil spill control, Mar. Pollut. Bull. 112 (2016) 46–52. doi:10.1016/j.marpolbul.2016.08.046.
[19] S.F. Soares, M.I. Rodrigues, T. Trindade, A.L. Daniel-da-Silva, Chitosan-silica hybrid nanosorbents for oil removal from water, Colloids Surfaces A Physicochem. Eng. Asp. 532 (2017) 305–313. doi:10.1016/j.colsurfa.2017.04.076.
[20] S. Zhang, T. Lü, D. Qi, Z. Cao, D. Zhang, H. Zhao, Synthesis of quaternized chitosan-coated magnetic nanoparticles for oil-water separation, Mater. Lett. 191 (2017) 128–131. doi:10.1016/j.matlet.2016.12.092.
[21] M. Rayner, D. Marku, M. Eriksson, M. Sjöö, P. Dejmek, M. Wahlgren, Biomass-based particles for the formulation of Pickering type emulsions in food and topical applications, Colloids Surfaces A Physicochem. Eng. Asp. 458 (2014) 48–62. doi:10.1016/j.colsurfa.2014.03.053.
[22] R. Aveyard, B.P. Binks, J.H. Clint, Emulsions stabilised solely by colloidal particles, Adv. Colloid Interface Sci. 100–102 (2003) 503–546. doi:10.1016/S0001-8686(02)00069-6.
[23] L. Payet, E.M. Terentjev, Emulsification and Stabilization Mechanisms of O/W Emulsions in the Presence of Chitosan, Langmuir. 24 (2008) 12247–12252. doi:10.1021/la8019217.
[24] X.-Y. Wang, M.-C. Heuzey, Chitosan-Based Conventional and Pickering Emulsions with Long-Term Stability, Langmuir. 32 (2016) 929–936. doi:10.1021/acs.langmuir.5b03556.
[25] Y. Yang, Z. Fang, X. Chen, W. Zhang, Y. Xie, Y. Chen, Z. Liu, W. Yuan, An Overview of Pickering Emulsions: Solid-Particle Materials, Classification, Morphology, and Applications, Front. Pharmacol. 8 (2017) 287. doi:10.3389/fphar.2017.00287.
[26] V. Calabrese, J.C. Courtenay, K.J. Edler, J.L. Scott, Pickering emulsions stabilized by naturally derived or biodegradable particles, Curr. Opin. Green Sustain. Chem. 12 (2018) 83–90.

doi:10.1016/j.cogsc.2018.07.002.
[27] D.J. French, P. Taylor, J. Fowler, P.S. Clegg, Making and breaking bridges in a Pickering emulsion, J. Colloid Interface Sci. 441 (2015) 30–38. doi:10.1016/j.jcis.2014.11.032.
[28] I. Kalashnikova, H. Bizot, P. Bertoncini, B. Cathala, I. Capron, Cellulosic nanorods of various aspect ratios for oil in water Pickering emulsions, Soft Matter. 9 (2013) 952–959. doi:10.1039/C2SM26472B.
[29] M. Matos, A. Marefati, R. Bordes, G. Gutiérrez, M. Rayner, Combined emulsifying capacity of polysaccharide particles of different size and shape, Carbohydr. Polym. 169 (2017) 127–138. doi:10.1016/j.carbpol.2017.04.006.
[30] C.S.K. Lin, L.A. Pfaltzgraff, L. Herrero-Davila, E.B. Mubofu, S. Abderrahim, J.H. Clark, A.A. Koutinas, N. Kopsahelis, K. Stamatelatou, F. Dickson, S. Thankappan, Z. Mohamed, R. Brocklesby, R. Luque, Food waste as a valuable resource for the production of chemicals, materials and fuels. Current situation and global perspective, Energy Environ. Sci. 6 (2013) 426. doi:10.1039/c2ee23440h.
[31] F.D. Romelle, A. Rani, R.S. Manohar, Chemical composition of some selected fruit peels, Eur. J. Food Sci. Technol. 4 (2016) 12–21.
[32] L.A. Pfaltzgraff, M. De bruyn, E.C. Cooper, V. Budarin, J.H. Clark, Food waste biomass: a resource for high-value chemicals, Green Chem. 15 (2013) 307–314. doi:10.1039/c2gc36978h.
[33] F. Meng, B. Yang, B. Wang, S. Duan, Z. Chen, W. Ma, Novel Dendrimerlike Magnetic Biosorbent Based on Modified Orange Peel Waste: Adsorption–Reduction Behavior of Arsenic, ACS Sustain. Chem. Eng. 5 (2017) 9692–9700. doi:10.1021/acssuschemeng.7b01273.
[34] B.H. Hameed, A.A. Ahmad, Batch adsorption of methylene blue from aqueous solution by garlic peel, an agricultural waste biomass, J. Hazard. Mater. 164 (2009) 870–875. doi:10.1016/j.jhazmat.2008.08.084.
[35] D. Sud, G. Mahajan, M. Kaur, Agricultural waste material as potential adsorbent for sequestering heavy metal ions from aqueous solutions – A review, Bioresour. Technol. 99 (2008) 6017–6027. doi:10.1016/j.biortech.2007.11.064.
[36] R. Diaz-Ruiz, M. Costa-Font, J.M. Gil, Moving ahead from food-related behaviours: an alternative approach to understand household food waste generation, J. Clean. Prod. 172 (2018) 1140–1151. doi:10.1016/j.jclepro.2017.10.148.
[37] S. Achinas, V. Achinas, G.J.W. Euverink, A Technological Overview of Biogas Production from Biowaste, Engineering. 3 (2017) 299–307. doi:10.1016/J.ENG.2017.03.002.
[38] J. González-Rivera, A. Spepi, C. Ferrari, C. Duce, I. Longo, D. Falconieri, A. Piras, M.R. Tinè, Novel configurations for a citrus waste based biorefinery: from solventless to simultaneous ultrasound and microwave assisted extraction, Green Chem. 18 (2016) 6482–6492. doi:10.1039/C6GC02200F.
[39] P. Putnik, D. Bursać Kovačević, A. Režek Jambrak, F. Barba, G. Cravotto, A. Binello, J. Lorenzo, A. Shpigelman, Innovative "Green" and Novel Strategies for the Extraction of Bioactive Added Value Compounds from Citrus Wastes—A Review, Molecules. 22 (2017) 680. doi:10.3390/molecules22050680.
[40] S. Thévenet, A. Wernicke, S. Belniak, G. Descotes, A. Bouchu, Y. Queneau, Esterification of unprotected sucrose with acid chlorides in aqueous medium: kinetic reactivity versus acyl- or alkyloxycarbonyl-group migrations, Carbohydr. Res. 318 (1999) 52–66. doi:10.1016/S0008-6215(99)00079-8.
[41] J.H. Bridson, W.J. Grigsby, L. Main, Synthesis and characterization of flavonoid laurate esters by transesterification, J. Appl. Polym. Sci. 129 (2013) 181–186. doi:10.1002/app.38731.
[42] M. Abdullah, S.H.A. Muhamad, S.N. Sanusi, S.I.S. Jamaludin, N.F. Mohamad, M.A.H. Rusli, Preliminary study of Oil Removal using hybrid Peel Waste: Musa Balbisiana and Citrus Sinensis, J. Appl. Environ. Biol. Sci. 6 (2016) 59–63.

[43] B. Doshi, E. Repo, J.P. Heiskanen, J.A. Sirviö, M. Sillanpää, Sodium salt of oleoyl carboxymethyl chitosan: A sustainable adsorbent in the oil spill treatment, J. Clean. Prod. 170 (2018) 339–350. doi:10.1016/j.jclepro.2017.09.163.
[44] J.W. Wang, M.H. Hon, Preparation and characterization of pH sensitive sugar mediated (polyethylene glycol/chitosan) membrane, J. Mater. Sci. Mater. Med. 14 (2003) 1079–1088. doi:10.1023/B:JMSM.0000004005.52762.ea.
[45] D. Zhang, W. Zhou, B. Wei, X. Wang, R. Tang, J. Nie, J. Wang, Carboxyl-modified poly(vinyl alcohol)-crosslinked chitosan hydrogel films for potential wound dressing, Carbohydr. Polym. 125 (2015) 189–199. doi:10.1016/j.carbpol.2015.02.034.
[46] M. Thirumavalavan, Y.-L. Lai, L.-C. Lin, J.-F. Lee, Cellulose-Based Native and Surface Modified Fruit Peels for the Adsorption of Heavy Metal Ions from Aqueous Solution: Langmuir Adsorption Isotherms, J. Chem. Eng. Data. 55 (2010) 1186–1192. doi:10.1021/je900585t.
[47] M.R. Mafra, L. Igarashi-Mafra, D.R. Zuim, É.C. Vasques, M.A. Ferreira, Adsorption of remazol brilliant blue on an orange peel adsorbent, Brazilian J. Chem. Eng. 30 (2013) 657–665. doi:10.1590/S0104-66322013000300022.
[48] R.L. Patale, V.B. Patravale, O,N-carboxymethyl chitosan–zinc complex: A novel chitosan complex with enhanced antimicrobial activity, Carbohydr. Polym. 85 (2011) 105–110. doi:10.1016/j.carbpol.2011.02.001.
[49] L. Bédouet, B. Courtois, J. Courtois, Methods for obtaining neutral and acid oligosaccharides from flax pectins, Biotechnol. Lett. 27 (2005) 33–40. doi:10.1007/s10529-004-6314-x.
[50] L.M.A. Silva, E.G. Alves Filho, R. Choze, L.M. Lião, G.B. Alcantara, 1H HRMAS NMR spectroscopy and chemometrics for evaluation of metabolic changes in citrus sinensis Caused by Xanthomonas axonopodis pv. citri, J. Braz. Chem. Soc. 23 (2012) 1054–1061. doi:10.1590/S0103-50532012000600009.
[51] C.R. de Oliveira, R.L. Carneiro, A.G. Ferreira, Tracking the degradation of fresh orange juice and discrimination of orange varieties: An example of NMR in coordination with chemometrics analyses, Food Chem. 164 (2014) 446–453. doi:10.1016/j.foodchem.2014.05.026.
[52] B. Gullón, M.I. Montenegro, A.I. Ruiz-Matute, A. Cardelle-Cobas, N. Corzo, M.E. Pintado, Synthesis, optimization and structural characterization of a chitosan–glucose derivative obtained by the Maillard reaction, Carbohydr. Polym. 137 (2016) 382–389. doi:10.1016/j.carbpol.2015.10.075.
[53] G. Kaptay, On the equation of the maximum capillary pressure induced by solid particles to stabilize emulsions and foams and on the emulsion stability diagrams, Colloids Surfaces A Physicochem. Eng. Asp. 282–283 (2006) 387–401. doi:10.1016/j.colsurfa.2005.12.021.
[54] D.J. McClements, C.E. Gumus, Natural emulsifiers — Biosurfactants, phospholipids, biopolymers, and colloidal particles: Molecular and physicochemical basis of functional performance, Adv. Colloid Interface Sci. 234 (2016) 3–26. doi:10.1016/j.cis.2016.03.002.
[55] S.. Shiao, V. Chhabra, A. Patist, M.. Free, P.D.. Huibers, A. Gregory, S. Patel, D.. Shah, Chain length compatibility effects in mixed surfactant systems for technological applications, Adv. Colloid Interface Sci. 74 (1998) 1–29. doi:10.1016/S0001-8686(97)00005-5.
[56] S.R. Valandro, P.C. Lombardo, A.L. Poli, C.E. Posakoda, C.C.S. Cavalheiro, Effect of Hydrocarbon Chain Length Surfactants on Particle Size of SWy-1 Montmorillonite Suspensions, Int. J. Basic Appl. Sci. 13 (2013) 1–6.
[57] S.W. Benner, V.T. John, C.K. Hall, Simulation Study of Hydrophobically Modified Chitosan as an Oil Dispersant Additive, J. Phys. Chem. B. 119 (2015) 6979–6990. doi:10.1021/acs.jpcb.5b01092.
[58] T. Jiao, X. Liu, J. Niu, Effects of sodium chloride on adsorption at different interfaces and aggregation behaviors of disulfonate gemini surfactants, RSC Adv. 6 (2016) 13881–13889. doi:10.1039/C5RA25727A.

[59] U.S. Schmidt, K. Schmidt, T. Kurz, H.-U. Endreß, H.P. Schuchmann, Pectins of different origin and their performance in forming and stabilizing oil-in-water-emulsions, Food Hydrocoll. 46 (2015) 59–66. doi:10.1016/j.foodhyd.2014.12.012.
[60] U.S. Schmidt, L. Schütz, H.P. Schuchmann, Interfacial and emulsifying properties of citrus pectin: Interaction of pH, ionic strength and degree of esterification, Food Hydrocoll. 62 (2017) 288–298. doi:10.1016/j.foodhyd.2016.08.016.
[61] S. Ghorbanizadeh, B. Rostami, Surface and Interfacial Tension Behavior of Salt Water Containing Dissolved Amphiphilic Compounds of Crude Oil: The Role of Single-Salt Ionic Composition, Energy & Fuels. 31 (2017) 9117–9124. doi:10.1021/acs.energyfuels.7b01394.
[62] D.A. Riehm, D.J. Rokke, P.G. Paul, H.S. Lee, B.S. Vizanko, A. V. McCormick, Dispersion of oil into water using lecithin-Tween 80 blends: The role of spontaneous emulsification, J. Colloid Interface Sci. 487 (2017) 52–59. doi:10.1016/j.jcis.2016.10.010.
[63] M.M. Kasprzak, A. Erxleben, J. Ochocki, Properties and applications of flavonoid metal complexes, RSC Adv. 5 (2015) 45853–45877. doi:10.1039/C5RA05069C.
[64] D.R. Alves, J.S.A. Carneiro, I.F. Oliveira, F. Façanha, A.F. Santos, C. Dariva, E. Franceschi, M. Fortuny, Influence of the salinity on the interfacial properties of a Brazilian crude oil–brine systems, Fuel. 118 (2014) 21–26. doi:10.1016/j.fuel.2013.10.057.
[65] R. Mohanram, C. Jagtap, P. Kumar, Isolation, screening, and characterization of surface-active agent-producing, oil-degrading marine bacteria of Mumbai Harbor, Mar. Pollut. Bull. 105 (2016) 131–138. doi:10.1016/j.marpolbul.2016.02.040.
[66] A.P. Kumar, A. Janardhan, B. Viswanath, K. Monika, J.-Y. Jung, G. Narasimha, Evaluation of orange peel for biosurfactant production by Bacillus licheniformis and their ability to degrade naphthalene and crude oil, 3 Biotech. 6 (2016) 43. doi:10.1007/s13205-015-0362-x.

Graphical abstract

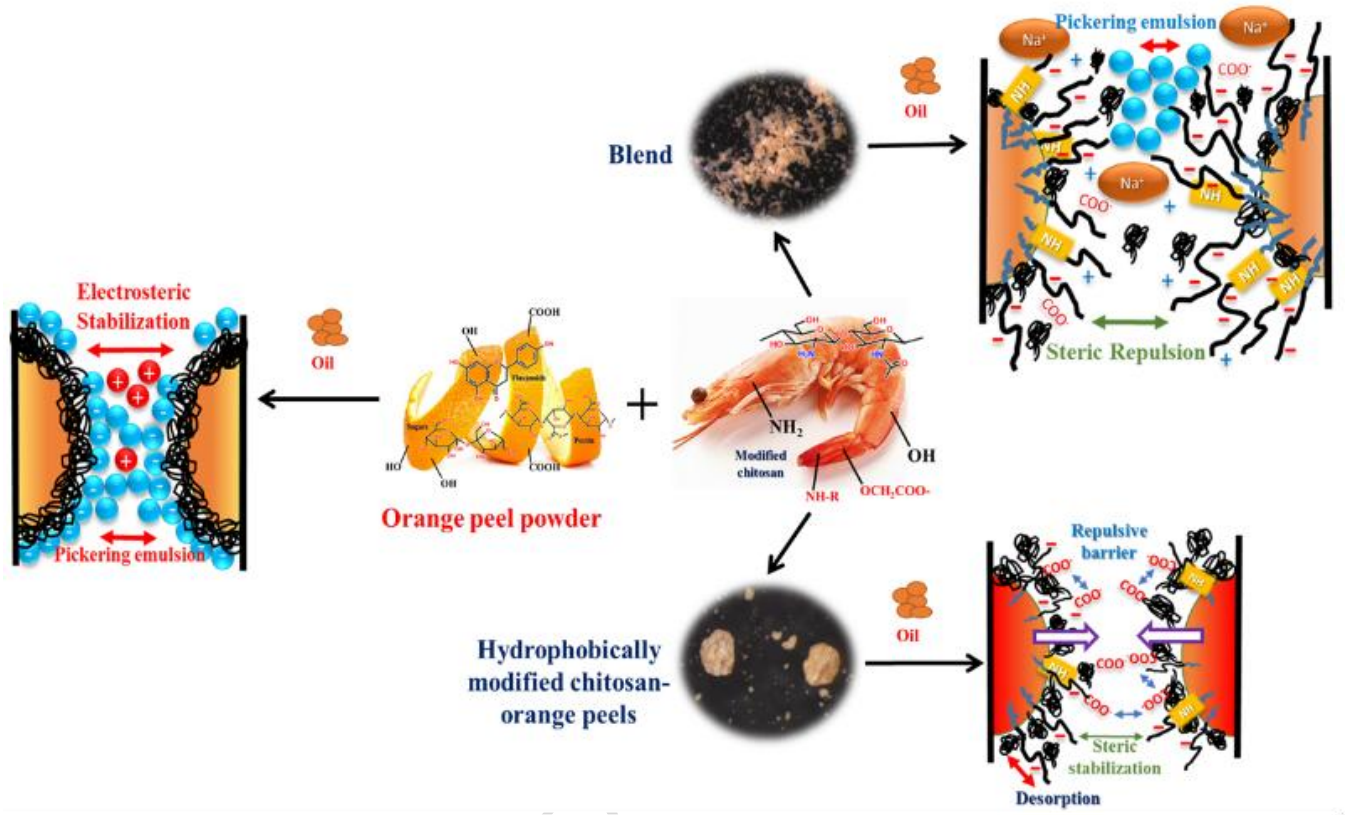

Highlights

- Powdered orange peels combined chitosan derivatives as an oil emulsifier
- Surface moieties of synthesized materials affects the emulsion formation rate
- Oil droplets stabilization rate was dependent on quality of water quality
- Changing pH altered the emulsion from gel-like to creamy
- Temperature affected oil droplets size and emulsion stability